# *Arabidopsis* m$^6$A demethylase activity modulates viral infection of a plant virus and the m$^6$A abundance in its genomic RNAs

Mireya Martínez-Pérez[a,1], Frederic Aparicio[a,1,2], Maria Pilar López-Gresa[a], Jose María Bellés[a], Jesus A. Sánchez-Navarro[a], and Vicente Pallás[a,2]

[a]Instituto de Biología Molecular y Celular de Plantas, Universitat Politécnica de Valencia–Consejo Superior de Investigaciones Científicas, 46022 Valencia, Spain

Edited by George E. Bruening, University of California, Davis, CA, and approved August 22, 2017 (received for review February 23, 2017)

**N$^6$-methyladenosine (m$^6$A) is an internal, reversible nucleotide modification that constitutes an important regulatory mechanism in RNA biology. Unlike mammals and yeast, no component of the m$^6$A cellular machinery has been described in plants at present. m$^6$A has been identified in the genomic RNAs of diverse mammalian viruses and, additionally, viral infection was found to be modulated by the abundance of m$^6$A in viral RNAs. Here we show that the *Arabidopsis thaliana* protein atALKBH9B (At2g17970) is a demethylase that removes m$^6$A from single-stranded RNA molecules in vitro. atALKBH9B accumulates in cytoplasmic granules, which colocalize with siRNA bodies and associate with P bodies, suggesting that atALKBH9B m$^6$A demethylase activity could be linked to mRNA silencing and/or mRNA decay processes. Moreover, we identified the presence of m$^6$A in the genomes of two members of the *Bromoviridae* family, alfalfa mosaic virus (AMV) and cucumber mosaic virus (CMV). The demethylation activity of atALKBH9B affected the infectivity of AMV but not of CMV, correlating with the ability of atALKBH9B to interact (or not) with their coat proteins. Suppression of atALKBH9B increased the relative abundance of m$^6$A in the AMV genome, impairing the systemic invasion of the plant, while not having any effect on CMV infection. Our findings suggest that, as recently found in animal viruses, m$^6$A modification may represent a plant regulatory strategy to control cytoplasmic-replicating RNA viruses.**

m6A | demethylase | ALKBH9B | plant virus | coat protein

N$^6$-methyladenosine (m$^6$A) is an internal, reversible nucleotide modification present in RNAs of mammals, insects, plants, yeast, and animal viruses that participates in RNA biology through diverse mechanisms such as regulation of mRNA stability (1, 2), translation (3, 4), nuclear export (5), exon splicing (6), and protein/RNA interactions (7).

In mammals, RNA m$^6$A methylation is catalyzed by a polyprotein complex composed of METTL3, METTL14, WTAP, KIAA1429, and several cofactors not yet identified (8–10). Removal of the m$^6$A is catalyzed by two RNA demethylases belonging to the AlkB family of nonheme Fe(II)/α-ketoglutarate (α-KG)-dependent dioxygenases, FTO, and ALKBH5 (5, 11). In addition, several proteins (YTHDF1, YTHDF2, YTHDF3, YTHDC, eiF3, and HNRNPC) bind to the m$^6$A-modified mRNAs to control their stability and translation (1, 2, 12, 13).

The internal m$^6$A modification has also been found in viral RNAs (vRNAs) of animal viruses that replicate either in the nucleus or in the cytoplasm, representing a mechanism for the regulation of the viral life cycle (14–19). Silencing of METTL3/14 decreased HIV-1 replication, whereas depletion of ALKBH5 enhanced the export of vRNAs from the nucleus and protein expression, which consequently increased viral replication (15, 16). However, hepatitis C virus (HCV) and Zika virus (ZIKV) infection were positively and negatively regulated by knockdown of METTL3/14 and ALKBH5 or FTO, respectively (17, 19). Further, depletion of YTHDF proteins promoted ZIKA and HCV vRNA expression (17, 19), while in the case of HIV-1, positive (18) and negative (15) effects on HIV-1 vRNA expression have been reported. Furthermore, the host machinery that controls m$^6$A modification detects viral infection and regulates gene expression by modulating the m$^6$A levels of host mRNAs (16, 17).

In contrast to mammals, very few studies on the function of m$^6$A modification have been reported in plants. Transcriptome-wide profiles in *Arabidopsis thaliana* detected the m$^6$A modification in over two-thirds of the mRNAs (20). A METTL3 homolog in *Arabidopsis* (MTA) has been identified that plays a critical role in plant development (21, 22). In addition, the *Arabidopsis* FIP37 protein, a plant homolog of WTAP, interacts in vitro and in vivo with MTA and is essential to mediate m$^6$A mRNA modification of key shoot meristem genes (21, 23). However, no demethylase or YTHFD plant activities have been described at present. The *Arabidopsis* genome contains 13 homologs of *Escherichia coli* AlkB (atALKBH1-10B) (24). Although their functional characterization has not been reported, a subcellular localization study showed that all of these proteins display a nucleocytoplasmic localization pattern except atALKBH1D, which localizes to the chloroplast as well, and atALKBH9B, which is exclusively cytoplasmic (24). Interestingly, an AlkB domain has been identified in the ORF of the replicase genes from diverse plant viruses. These domains were found to be functional in removing m$^1$A and m$^3$C modifications from RNA and DNA in vitro, suggesting that the replicase proteins

## Significance

**N$^6$-methyladenosine (m$^6$A) modification has been found to constitute an important regulatory mechanism in RNA biology. Unlike mammals and yeast, no component of the m$^6$A cellular machinery has been described in plants at present. Although the influence of the m6A cellular machinery has been suspected to occur in the plant virus cycle, it has never been proved. Here we have identified a plant protein with m$^6$A demethylase activity (atALKBH9B) and demonstrate that this protein removes m$^6$A modification from RNA in vitro. Remarkably, we found that m$^6$A abundance on the viral genome of alfalfa mosaic virus is influenced by atALKBH9B activity and regulates viral infection. This study extends the vast repertoire that plants exploit to control cytoplasmic-replicating RNA viruses.**

Author contributions: F.A. and V.P. designed research; M.M.-P., F.A., and M.P.L.-G. performed research; M.M.-P., F.A., M.P.L.-G., J.M.B., and J.A.S.-N. contributed new reagents/analytic tools; M.M.-P., F.A., J.M.B., and J.A.S.-N. analyzed data; and M.M.-P., F.A., and V.P. wrote the paper.

The authors declare no conflict of interest.

This article is a PNAS Direct Submission.

[1]M.M.-P. and F.A. contributed equally to this work.

[2]To whom correspondence may be addressed. Email: faparici@ibmcp.upv.es or vpallas@ibmcp.upv.es.

This article contains supporting information online at www.pnas.org/lookup/suppl/doi:10.1073/pnas.1703139114/-/DCSupplemental.

play a role in reversing methylation modifications in the viral genomes (25).

In this work, we identified a plant protein with m$^6$A demethylase activity (atALKBH9B) in *Arabidopsis* and showed that the protein interacts with the coat protein (CP) of alfalfa mosaic virus (AMV) in the cell cytoplasm. The AMV genome consists of three single-stranded RNAs of positive sense polarity. RNAs 1 and 2 encode the replicase subunits, whereas RNA 3 encodes the movement protein and serves as a template for the synthesis of nonreplicating subgenomic RNA 4 (sgRNA 4), which encodes the CP (26). The AMV CP localizes to both the nucleus/nucleous and the cytoplasm (27), although viral replication occurs in the cytoplasm, most probably associated with the tonoplast membrane (28). We found that an *Arabidopsis* knockout mutation of atALKBH9B negatively affects virus accumulation and systemic invasion, correlating with increased levels of m$^6$A of the vRNAs. Our results show that the viral genome methylation state plays a key role in the life cycle of a plant virus.

## Results

***Arabidopsis* atALKBH9B Interacts with the CP and the Viral RNA of AMV.** The CP of AMV is a multifunctional protein that participates in replication, translation, viral movement, and encapsidation (26, 29), which most probably implies that this protein interacts with host factors involved in diverse cellular functions (30, 31). A yeast two-hybrid (Y2H) screen, using the CP as bait and an *Arabidopsis* leaf-specific cDNA library as the prey, was performed to identify host proteins that interact with the AMV CP. Several clones containing part of the *atALKBH9B* gene (at2g17970) ORF were found to grow on interaction minimal synthetic selective medium (Fig. S1*A*). To validate the original Y2H screening, the full-length *atALKBH9B* ORF was fused to the activation domain (pAD plasmid) and transformed into yeast cells expressing the AMV CP fused to the binding domain (pBD plasmid). After growth at 28 °C for 5 d on interaction selective medium, we found that the AMV CP specifically interacted with atALKBH9B but not with the empty pBD vector or the one expressing the Gal4 binding domain fused with lamin (pBD:LAM) (Fig. 1*A*). To corroborate this interaction, histidine-tagged atALKBH9B (His-atALKBH9B) and the N-terminal fragment of YFP (His-NYFP) were expressed in *E. coli* and purified by Ni-NTA agarose chromatography. Before the elution step, Ni-NTA columns containing his-tagged proteins were incubated with purified AMV virions. Western blot analysis using anti-CP antibody of eluates after incubation with viral particles showed that virions interacted with atALKBH9B but not with NYFP (Fig. S1*B*). To confirm that the CP–atALKBH9B interaction occurs in planta we used bimolecular complementation (BiFC) analysis. Confocal laser scanning microscopy (CLSM) images showed that reconstituted YFP fluorescence formed discrete granules in cells of *Nicotiana benthamiana* infiltrated with atALKBH9B plus AMV CP but not when the host protein was coinfiltrated with the C-terminal fragment of YFP alone (CYFP) (Fig. 1*B*). Finally, a Northwestern blot assay demonstrated that atALKBH9B interacts with viral RNA, showing that the protein has RNA binding activity (Fig. 1*C*).

***Arabidopsis* atALKBH9B Activity Modulates AMV Infection.** To investigate possible roles for atALKBH9B in virus infection, we searched for T-DNA insertions in *atALKBH9B*. We identified a homozygous $T_3$ line in the Nottingham *Arabidopsis* Stock Centre (N671317; SALK_015591, ecotype Col-0) with a T-DNA insertion in exon 4 (Fig. 2*A*). Absence of atALKBH9B mRNA expression was confirmed by RT-PCR with gene-specific primers (Fig. 2*B*). To determine whether reduced levels of atALKBH9B affect virus infection, WT Col-0 and *atalkbh9b* plants were inoculated with AMV viral particles. Total RNA and proteins were extracted and vRNA and CP accumulation were analyzed at 3 and 6 d postinoculation (dpi) by Northern and Western blots using a digoxigenin-labeled probe to detect the vRNAs (DigAMV) and a specific anti-CP antibody, respectively. We found that levels of both vRNAs and CP were clearly reduced in *atalkbh9b* compared with WT plants (Fig. 2 *C* and *D* and Fig. S2), indicating that viral accumulation is impaired in *atalkbh9b* plants. To analyze AMV systemic movement, total RNA extracted from upper noninoculated floral stems were blotted onto nylon membranes, and vRNAs were detected with DigAMV. Fig. 2*E* shows that only 11% of *atALKBH9B* plants were systemically infected at 14 dpi, while this percentage reached 100% in WT plants. Overall, these results indicate that atALKBH9B positively regulates AMV infection.

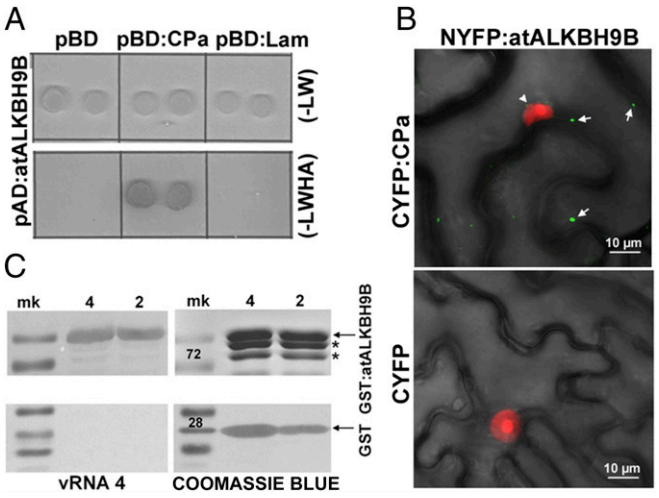


**Fig. 1.** atALKBH9B interacts with the CP of AMV in vitro and in vivo and with the viral RNA. (*A*) Yeast two-hybrid analysis of the interaction between AMV CP and atALKBH9B. Interacting colonies were identified by growth after 5 d on medium lacking leucine, tryptophan, histidine, and adenine (–LWHA). (*B*) BiFC images of epidermal cells coinfiltrated with the indicated constructs. YFP reconstitution was found to form discrete granules in the cytoplasm (arrows). Fibrillarin fused to the mCherry protein was used to identify the cell nuclei (arrowhead). Pictures are the overlapped images of green, red, and transmitted channels. (*C*) Analysis of the RNA binding activity of atALKBH9B by Northwestern blot assay. Duplicate membranes with purified GST:atALKBH9B (*Upper*) or GST proteins (*Lower*) (4 and 2 μg) were incubated with viral RNA 4 (*Left*) to show the RNA binding activity or stained with Coomassie blue (*Right*) to confirm the presence of the proteins. Positions of full-length GST and GST:atALKBH9B proteins are indicated by arrows. Asterisks denote truncated GST:atALKBH9B.

**atALKBH9B Localizes to Cytoplasmic Bodies.** atALKBH9B is one of the 13 homologs of *E. coli* AlkB, and it is the only one that is uniquely located in the cytoplasm (24). To determine more precisely the atALKBH9B subcellular localization, we transiently expressed translational fusions with GFP (GFP:atALKBH9B and atALKBH9B:GFP) by agroinfiltration in *N. benthamiana* leaves. CLSM images showed that atALKBH9B:GFP was localized as a diffuse pattern throughout the cytoplasm, while GFP:atALKBH9B was accumulated in small cytoplasmic granules and filaments (Fig. S3). We next performed a sequence similarity analysis, which showed that five *Arabidopsis* AlkB homologs, including atALKBH9B, grouped in the same branch with human ALKBH5 (Fig. S4). Hence, these proteins might be orthologous to the human protein and other prospective m$^6$A demethylases. It has been proposed that m$^6$A methylation functions in the cytoplasm, serving as a reversible tag to direct mRNAs to processing bodies (P bodies) (12). Moreover, several studies have demonstrated that P bodies dynamically associate with siRNA bodies, and the latter are implicated in posttranscriptional gene silencing (PTGS) through the synthesis of dsRNAs to generate siRNAs (32, 33). We reasoned that atALKBH9B-forming granules might be related to siRNA

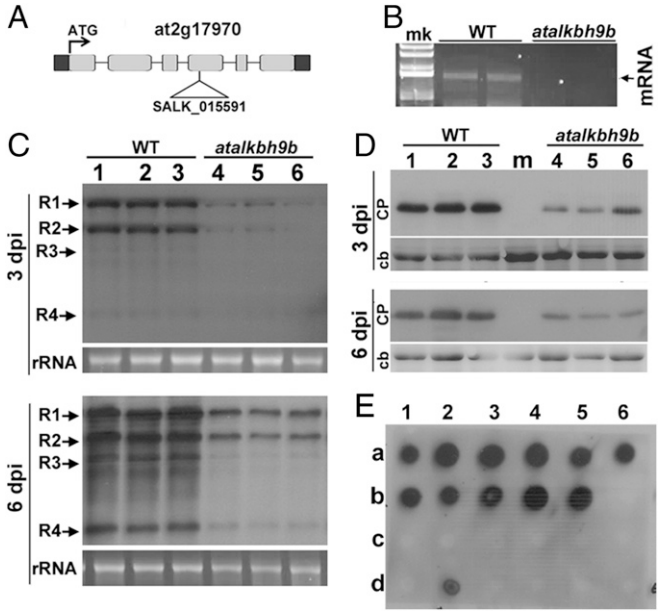


**Fig. 2.** AMV infection is impaired in *atalkbh9b* plants. (*A*) Annotated genomic *atALKBH9B* gene structure showing the exons (gray boxes) and location of the T-DNA insertion (SALK_015591). (*B*) Agarose gel electrophoresis of RT-PCR products produced with specific primers to amplify the full-length mRNA of the *atalkbh9b* gene from WT and *atalkbh9b* plants. The position of the mRNA is indicated on the *Right*. (*C* and *D*) Representative Northern and Western blots from inoculated leaves at 3 and 6 dpi of three WT and *atalkbh9b* plants. Positions of the vRNAs and CP are indicated on the *Left*. Ethidium bromide and Coomassie blue staining of ribosomal RNAs and total protein extracts (rRNA and cb, respectively) were used as RNA and protein loading controls. (*E*) Dot-blot hybridization of upper noninoculated floral stems to determine the extent of viral systemic movement. Dots in rows *a* and *b* correspond to WT plants; dots in *c* and *d* correspond to *atalkbh9b* plants. Samples *b*6 and *d*6 are healthy WT and *atalkbh9b* plants used as negative controls.

and/or P bodies. To test this hypothesis, we performed colocalization experiments in mock and AMV-infected *N. benthamiana* leaves by coexpressing atALKBH9B with DCP1 (a decapping enzyme located in P bodies) and SGS3 (a component of siRNA bodies) (32, 34) fused to fluorescent proteins. CLSM images showed that, in both healthy and infected tissues, atALKBH9B granules perfectly colocalized with siRNA bodies, whereas ∼40% of the atALKBH9B granules were spatially associated with P bodies (Fig. 3*A* and Fig. S5). These results suggest that atALKBH9B might be a new component of siRNA bodies and P bodies.

Recently, the nonsense-mediated mRNA decay system (NMD) has been proposed to work as viral restriction mechanism in plants (35). The regulator of nonsense transcripts 1 (UPF1) is a critical component of this RNA quality control system and is found to be linked to P bodies (36). To shed light on which viral functions might be modulated by m$^6$A modification, we have analyzed the impact of the NMD in AMV infection. Subcellular localization of UPF1 by CLMS showed that the construct atUPF1:GFP also formed cytoplasmic discrete granules colocalizing with GFP:atALKBH9B (Fig. 3*B*). Further, the analysis of vRNAs accumulation revealed a significant enhancement in systemic leaves of *Arabidopsis upf1.5* mutant plants (at5g47010; SALK_112922) (Fig. 3*C*). Altogether, our results suggest that atALKBH9B might be a new component of siRNA bodies and P bodies and, as found in other plant viruses (35), NMD would restrict AMV infection.

**atALKBH9B Catalyzes m$^6$A Demethylation of RNA in Vitro.** To assay the m$^6$A demethylation activity of atALKBH9B, the protein was fused to the glutathione S-transferase (GST) protein (GST:atALKBH9B) and purified from *E. coli* using the GST purification system. GST:atALKBH9B or GST alone was incubated with a synthetic single-stranded RNA oligonucleotide (ssRNA) with a single specifically incorporated m$^6$A, followed by digestion to nucleosides and ultra-performance liquid chromatography–photodiode detector–quadrupole/time-of-flight–mass spectrometry (UPLC-PDA-TOF-MS) analysis. We found that GST:atALKBH9B almost completely demethylates m$^6$A in the ssRNA substrate (Fig. 4 *A* and *B*). Therefore, atALKBH9B is a protein described in plants with ssRNA m$^6$A demethylase activity.

**m$^6$A Abundance in AMV vRNAs Correlates with Viral Fitness.** Given that atALKBH9B has been shown to possess m$^6$A demethylase activity and that its depletion influences AMV infection, we investigated the presence of the m$^6$A modification in AMV vRNAs. Total RNA was purified from *Arabidopsis* WT AMV-infected plants, and an RNA immunoprecipitation assay (RIP) using the anti-m$^6$A antibody and immunoglobulin-A was performed to immunoprecipitate the m$^6$A-modified RNAs. Subsequent hybridization of RIP products with the DigAMV probe clearly detected the presence of the AMV vRNAs (Fig. 4 *C* and *D*). These results demonstrate that in *Arabidopsis*, adenosine residues in the AMV genome become modified to m$^6$A during the infection process. We next determined whether atALKBH9B depletion in *atalkbh9b* plants modulates m$^6$A levels in the AMV genome. In this case, vRNAs extracted from AMV particles isolated from WT or *atalkbh9b* plants were electrophoresed in agarose gels, transferred to nylon membranes, and immunoblotted using the m$^6$A antibody (Fig. S6). In parallel, vRNAs were digested to single nucleosides and the m$^6$A abundance was quantified by UPLC-PDA-Tof-MS. The m$^6$A/adenosine ratio (m$^6$A/A) was reduced ∼35% in WT

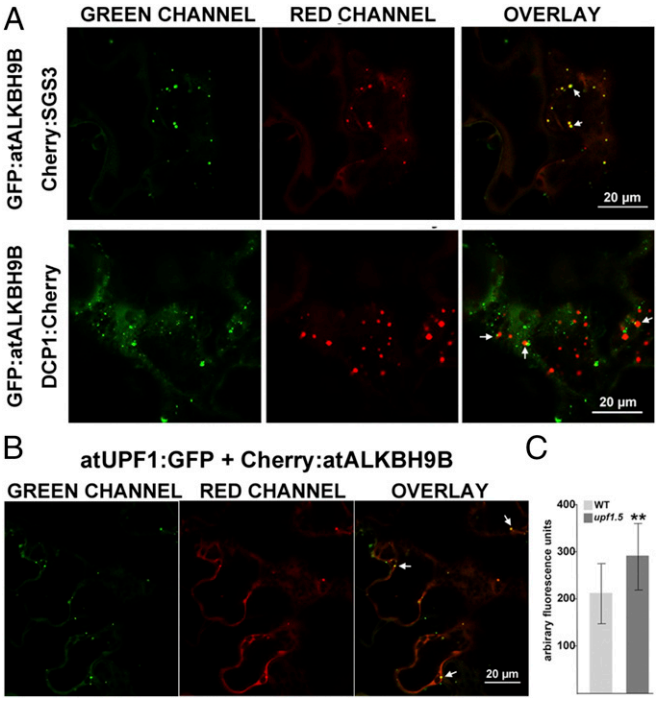


**Fig. 3.** The atALKBH9B protein colocalizes with siRNA-body/P-body components in noninfected tissues. (*A* and *B*) Confocal laser scanning microscope (CLSM) images of *N. benthamiana* leaf epidermal cells coinfiltrated with the DNA constructs indicated *Above* the images. Overlay panels are the superposition of images from the green and red channels. Arrowheads indicate granules with both proteins. (*C*) vRNAs accumulation in *upf1.5* mutant with respect to WT. SD values are shown. Asterisks indicate significant differences from the WT (**$P < 0.01$) using the *t* test ($n = 20$).

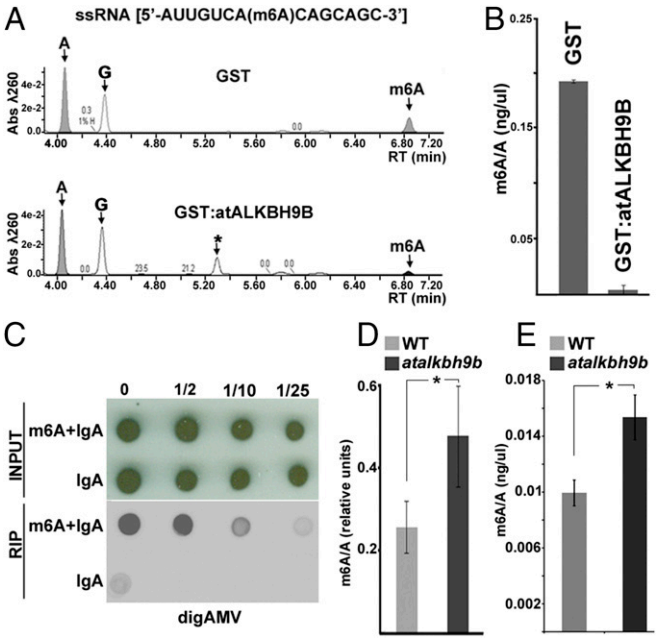


**Fig. 4.** atALKBH9B catalyzes demethylation of m$^6$A in ssRNA in vitro and modulates methylation of vRNAs. (*A*) Representative UPLC-PDA-Q/TOF-MS chromatogram showing the retention times of the nucleosides adenosine (A) and N$^6$-methyladenosine (m$^6$A) after incubation of the m$^6$A-containing ssRNA substrate with GST:atALKBH9B and GST as the negative control. The peak (G) corresponds to the nucleoside guanosine. The peak denoted as (*) could not be unequivocally identified although it was determined to present a molecular weight of 343 with a maximum absorption at 261 nm. (*B*) Graph representing the demethylation activity in three independent experiments. (*C*–*E*) Genomic AMV RNAs are m$^6$A hypermethylated in *atalkbh9b* plants. (*C*) RIP of vRNAs with a specific anti-m$^6$A antibody. Total RNA extracted from WT plants infected with AMV was incubated with anti-m$^6$A plus IgA or IgA alone. Dilutions of the immunoprecipitated RNAs (indicated on *Top*) were blotted on nylon membranes and the vRNAs were detected with DigAMV. (*D*) Average ratios of m$^6$A in vRNAs obtained by quantification of m$^6$A on three different Northwestern blots from AMV-infected WT and *atalkbh9b* plants. (*E*) Graphic showing the average m$^6$A/A ratios obtained by UPLC-Q-Tof-MS after digestion of vRNAs extracted from virions purified from AMV-infected WT and *atalkbh9b* plants. In *B*, *D*, and *E* error bars represent the SEM and asterisks indicate significant differences from the WT (*$P < 0.05$) using the *t* test ($n = 3$).

compared with *atalkbh9b* plants (Fig. 4*E*), indicating that depletion of atALKBH9B correlates with hypermethylation of the AMV vRNAs.

Finally, we performed a methylated RNA immunoprecipitation sequencing (MeRIP-seq) experiment to map m$^6$A sites within the AMV genome. For this, vRNAs extracted from viral particles isolated from *atalkbh9b* AMV-infected plants were immunoprecipitated with an m$^6$A-specific antibody and RNAs from input, bead-only control and MeRIP-seq samples were used to generate RNA sequence libraries. We identified six discrete peaks distributed along the AMV genome, which contained three of the common m$^6$A consensus motifs [(G,A,U)/(G,A)/A/C/(A,C,U)], [(A,C)/G/A/C/(G,U)] and [UGAC] (Fig. S7).

**m$^6$A Is Present in the Genomic RNAs of Other Members of the *Bromoviridae* Family.** Since m$^6$A appears to regulate AMV infection, we asked whether other viruses in the *Bromiviridae* family might also be influenced by this modification. We chose cucumber mosaic virus (CMV), the type member of the genus *Cucumovirus*, which infects *Arabidopsis* and is not closely related to AMV. First, the presence of m$^6$A was examined in CMV vRNAs by RIP from total RNA of WT CMV-infected plants using the m$^6$A antibody. Hybridization of RIP products with the DigCMV probe showed that the CMV genome contains m$^6$A as well (Fig. 5*A*). We then evaluated whether, similar to AMV, atALKBH9B activity might influence viral infectivity and/or m$^6$A modification in CMV vRNAs. To address this, total RNA was isolated from upper floral stems to look for systemic viral movement, and blot hybridization with the DigCMV probe showed that 100% of *atALKBH9B* plants were systemically infected by the virus (Fig. 5*B*). We also extracted vRNAs from viral particles isolated from WT and *atalkbh9b* plants infected with CMV. After digestion to single nucleosides, UPLC-PDA-Tof-MS showed no significant differences in the m$^6$A/A ratios in purified vRNAs from WT compared with *atALKBH9B* plants (Fig. 5*C*). Therefore, the CMV genome contains m$^6$A, but the methylation levels of vRNAs and viral infection are not regulated by atALKBH9B. We hypothesized that our findings might correlate with a lack of interaction between atALKBH9B and the CMV CP; hence, this interaction was investigated by Y2H analysis. Growth on interaction selective medium of yeast cells coexpressing both proteins showed that the viral protein fails to interact with atALKBH9B in vivo (Fig. 5*D*). Interestingly, we found that atALKBH9B interacts with the CP of *Prunus* necrotic ringspot virus (PNRSV) (Fig. 5*D*), a virus that is functionally and phylogenetically closely related to AMV (37, 38). Unfortunately, since *Arabidopsis* is not a host for PNRSV, we could not assay the virus infectivity in *atalkbh9b* plants. This finding suggests that atALKBH9B may regulate the viral life cycle of other *Bromoviridae* family members.

## Discussion

In the last few years, m$^6$A modification has emerged as an important mechanism to regulate mRNA biology (1, 2, 4–7). Components of this regulatory system (methyltransferases, demethylases, and

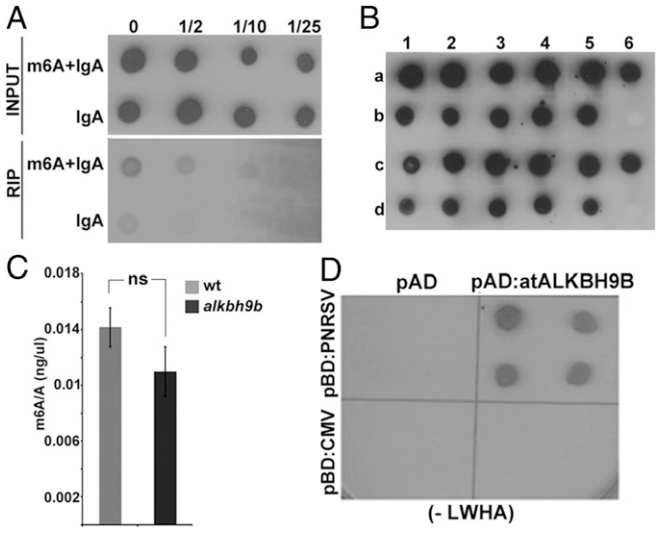


**Fig. 5.** CMV genomic RNAs contain the m$^6$A modification. (*A*) Detection of the m$^6$A modification in CMV by RIP of viral RNAs with a specific anti-m6A antibody plus IgA or IgA alone. Dilutions of the immunoprecipitated RNAs (indicated on *Top*) were blotted on nylon membranes and vRNAs were detected with DigCMV. (*B*) Graphic showing the average m$^6$A/A ratios obtained by UPLC-Q-Tof-MS after digestion of vRNAs extracted from virions purified from CMV-infected WT and *atalkbh9b* plants. Error bars represent SEM; ns, no significant differences ($P > 0.05$) from the WT using the *t* test ($n = 3$). (*C*) CMV systemic infection is not affected in *atalkbh9b* plants. Dot-blot hybridization of floral stems to analyze systemic viral movement. Samples *b*6 and *d*6 are the negative controls. Dots in rows *a* and *b* correspond to WT plants; dots in *c* and *d* correspond to *atalkbh9b* plants. (*D*) Yeast two-hybrid analysis of the interaction between CPs of CMV and PNRSV with atALKBH9B. Interacting colonies were identified by growth after 5 d on medium lacking leucine, tryptophan, histidine, and adenine (–LWHA). ns, not significant.

protein effectors) have been identified in mammals and yeast (12). Several recent studies have shown that $m^6A$ modification is also a conserved feature of mRNA in plants (20, 39), and that it plays a critical regulatory role in plant development (21–23). However, as far as we know, only two components of the methylase complex, MTA and FIP37, have been identified at present (21, 23). In this work, using a biochemical test, we demonstrate that atALKBH9B possesses $m^6A$ demethylase activity toward single-stranded RNA in vitro, and similar to the results of a previous study, we found that this protein localizes exclusively to the cytoplasm (24). Several studies have previously reported the presence of the cellular machinery controlling $m^6A$ modification in the cytoplasm of mammalian cells (17, 19,). Thus, atALKBH9B may be a new component of the cellular machinery controlling $N^6$ methylation of adenosine in plant mRNAs, and similar to the situation in mammals, $m^6A$ modification could take place in the cytoplasm after the export of mRNAs from the nucleus.

A detailed examination showed that atALKBH9B forms discrete granules either in healthy or infected tissues that colocalize with SGS3 and UPF1, and some of these granules presented a spatial association with DCP1. SGS3 and DPC1 are components of siRNA bodies and P bodies, respectively (33, 34), whereas that UPF1 is transported from the cytoplasm to P bodies by SMG7 (36). In the cytoplasm, binding of different proteins to $m^6A$ mediates host mRNA destination. For instance, binding of YTHDF1 or eIF3 has been found to favor mRNA translation (3, 4), whereas the binding of HNRNPC regulates mRNA degradation (7), and YTHDF2 directs $m^6A$-marked mRNAs to P bodies for RNA decay (4). RNA turnover in P bodies and PTGS in siRNA bodies are conserved eukaryotic mechanisms to regulate mRNA integrity that have been found to be functionally and spatially associated (33, 40). Our findings suggest that atALKBH9B $m^6A$ activity might be linked to mRNA silencing and the mRNA decay processes. In this sense, we found that NMD, a surveillance system linked to P bodies proposed to work as viral restriction mechanism in plants, could act on AMV infection, since UPF1 depletion increased viral accumulation (35).

Recent studies have shown that the $m^6A$ machinery modifies the viral RNA genomes of several animal viruses belonging to the *Flaviviridae* family, indicating that $m^6A$ modification is a conserved mark that regulates viral infection (17, 19). In this paper, we report that adenosines in the genomes of AMV and CMV are also modified to $m^6A$, suggesting that this feature is a conserved phenomenon in viruses that replicate in the cytoplasm of both mammalian and plant cells. In the case of AMV, we showed that AMV accumulation was reduced in inoculated leaves of *atalkbh9b* plants, and systemic infection of the plant was also severely impaired. Moreover, AMV genomic RNAs presented higher $m^6A$ levels in these mutant plants, providing evidence that $m^6A$ modification negatively affects viral infection. These findings are in agreement with those recently reported for HCV and ZIKV, in which viral infections are regulated by $m^6A$ modification of their genomic RNAs. Specifically, knockdown of *ALKBH5* and *FTO* increased $m^6A$ abundance in the ZIKV genome, negatively affecting the viral titer (17), while depletion of FTO but not ALKBH5 decreased the production of infectious virus (19). Thus, the host RNA methyltransferase machinery may represent an additional host regulatory mechanism to counter infection by some plant viruses.

Gokhale et al. (19) proposed that regulation of $m^6A$ abundance in genomic RNAs of HCV would allow the virus to replicate at low rates, evading the host immune system and enabling the establishment of persistent infections. In plants, a conserved AlkB domain in the genomes of several single-stranded RNA plant viruses belonging to the *Flexiviridae* family has been identified (25, 41). Furthermore, a functional characterization analysis showed that these viral AlkB domains repaired deleterious RNA genome methylation damage, suggesting that this domain may be biologically relevant in preserving the viability of the viral genome (25). Interestingly, most of the viruses containing this AlkB domain infect woody or perennial plants, where they have to establish infections that persist for years (25, 42). In the case of AMV, a similar scenario could occur, since alfalfa (*Medicago sativa*) plants, its natural host, are generally maintained for a minimum of 5 y before the crop is replanted (42). However, unlike viruses in the *Flexiviridae* family, the AMV genome lacks the Alkb domain, so the virus may have the ability to usurp this host function for its long-term accumulation.

We found that the CMV genome also contains $m^6A$, but differs from AMV in that neither $m^6A$ vRNA abundance nor virus infection was modified in *atalkbh9b* plants compared with WT plants. Remarkably, the CMV CP did not interact with atALKBH9B in vivo. An important difference between AMV and CMV is that, whereas the latter can replicate in the absence of its CP (43), the CP of AMV is a multifunctional protein that interacts with a variety of host factors and is indispensable for replication and translation (26–29). Thus, it may be possible that the interaction between atALKBH9B and the CP is essential to usurp atALKBH9B activity.

But on the other hand, the *Arabidopsis* genome encodes five putative demethylase orthologs, so a protein different from atALKBH9B could very well participate in the CMV $m^6A$ regulation process. In fact, it has been reported that depletion of FTO negatively affects HCV infection, while depletion of ALKBH5 has no effect on the HCV cycle (19). Finally, we cannot rule out the possibility that $m^6A$ modification does not influence CMV viral infection per se.

## Materials and Methods

**Analysis of GST:atALKBH9B-Viral RNA Interaction by Northwestern Assay.** Dilutions of GST or GST:ALKBH9B purified proteins were electrophoresed in 12% SDS/PAGE and transferred to PDVF membranes. Membranes were incubated overnight at 4 °C (10 mM Tris·HCl pH 7.5, 1 mM EDTA, 0.1 M NaCl, 0.0005% Triton X). After two washes of 5 min each with the same buffer, membranes were incubated with 20 mL of buffer B (10 mM Tris·HCl pH 7.5, 1 mM EDTA, 0.1 M NaCl) containing 50 ng/μL of the AMV RNA 4 labeled with digoxigenin for 2 h at 25 °C. Then digoxigenin detection procedures were carried out as detailed in *SI Materials and Methods*.

**BiFC and Subcellular Localization Study.** *atALKBH9B* and *atUPF1* ORFs were amplified with specific primers designed for cloning using the Gateway System (Invitrogen) and recombined into binary destination vectors expressing the fluorescent proteins mCherry or GFP for subcellular localization studies and the N-terminal part of the YFP for BiFC analysis, following manufacturer recommendations (GFP:atALKBH9B, atALKBH9B:GFP; NYFP:atALKBH9B, atUPF1:GFP). For details, see *SI Materials and Methods*.

**Virus Isolation and Viral Genomic RNA Purification and Rip Using m6A Antibody.** Virus purification was performed following PEG protocol with some modifications (*SI Materials and Methods*). For vRNAs purification, pellets were directly resuspended in 1 mL of RiboZol reagent (Amresco) and RNA extraction was carried out following manufacturer recommendations.

RNAs with $m^6A$ modification were immunoprecipitated as previously reported with some modifications as detailed in *SI Materials and Methods*.

**Purification of atALKBH9B Protein.** *atALKBH9B* was subcloned into pGEX-KG (GE Healthcare Life Sciences) to generate a construct with atALKBH9B fused to the C-terminal part of the GST. GST and GST:atALKBH9B proteins were expressed in BL21 (DE3) *E. coli* cells and purified with glutathione sepharose 4B beads (GE Healthcare Life Sciences) following manufacturer recommendations. All of the protein purification procedures were performed at 4 °C.

**In Vitro m6A Demethylation Assays.** The m6A demethylase activity assay was performed by incubating 2.5 μg of GST or GST:ALKBH9B proteins and 1 μg of $m^6A$ monomethylated ssRNA (Dharmacon, Inc.) oligonucleotide for 3 h at 25 °C in a reaction mixture containing 50 mM of Hepes buffer (pH 7.0), 10 μM α-ketoglutarate, 100 μM L-ascorbic acid ascorbate, 20 μM (NH4)2Fe(SO4) 2·6H2O. Finally, reactions were quenched by heating at 95 °C for 10 min. UPLC-PDA-Tof-MS analysis of vRNAs and ssRNA oligonucleotide demethylation were performed as described in *SI Materials and Methods*.

MICROBIOLOGY

**MeRip-Seq.** Immunoprecipitation of $m^6A$ RNA fragments was performed using 200 μg of purified vRNAs as previously described (44). For details, see *SI Materials and Methods*.

**ACKNOWLEDGMENTS.** We thank L. Corachan for her excellent technical assistance, Dr. Emilio Martinez de Alba and Dr. Christophe Rizenthaler for kindly providing GFP:SGS3 and DCP2:mCherry plasmids, Prof. John W. S. Brown for providing a plasmid containing the ORF of atUPF1, and the Bioinformatics Core Service at the Instituto de Biología Molecular y Celular de Plantas (IBMCP) for the support provided in the data analysis. UPLC-PDA-Q/TOF-MS analyses were performed by the Metabolic Analysis Department of the IBMCP. F.A. and M.M.-P. were recipients of Contract RYC-2010-06169 from the Ramón y Cajal Program of the Ministerio de Educación y Ciencia, and Predoctoral Contract FPI-2015-072406 from the Subprograma FPI-MINECO (Formación de Personal Investigador–Ministerio de Economía y Competitividad), respectively. This work was supported by Grant BIO2014-54862-R from the Spanish granting agency Dirección General de Investigación Científica y Técnica and the Prometeo Program (GV2015/010) from the Generalitat Valenciana.

1. Wang X, et al. (2014) N6-methyladenosine-dependent regulation of messenger RNA stability. *Nature* 505:117–120.
2. Xu C, et al. (2014) Structural basis for selective binding of m6A RNA by the YTHDC1 YTH domain. *Nat Chem Biol* 10:927–929.
3. Meyer KD, et al. (2015) 5′-UTR m(6)A promotes cap-independent translation. *Cell* 163: 999–1010.
4. Wang X, et al. (2015) N6-methyladenosine modulates messenger RNA translation efficiency. *Cell* 161:1388–1399.
5. Zheng G, et al. (2013) ALKBH5 is a mammalian RNA demethylase that impacts RNA metabolism and mouse fertility. *Mol Cell* 49:18–29.
6. Zhao X, et al. (2014) FTO-dependent demethylation of N6-methyladenosine regulates mRNA splicing and is required for adipogenesis. *Cell Res* 24:1403–1419.
7. Liu N, et al. (2015) N(6)-methyladenosine-dependent RNA structural switches regulate RNA-protein interactions. *Nature* 518:560–564.
8. Liu J, et al. (2014) A METTL3-METTL14 complex mediates mammalian nuclear RNA N6-adenosine methylation. *Nat Chem Biol* 10:93–95.
9. Ping X-L, et al. (2014) Mammalian WTAP is a regulatory subunit of the RNA N6-methyladenosine methyltransferase. *Cell Res* 24:177–189.
10. Schwartz S, et al. (2014) Perturbation of m6A writers reveals two distinct classes of mRNA methylation at internal and 5′ sites. *Cell Rep* 8:284–296.
11. Jia G, et al. (2011) N6-methyladenosine in nuclear RNA is a major substrate of the obesity-associated FTO. *Nat Chem Biol* 7:885–887.
12. Fu Y, Dominissini D, Rechavi G, He C (2014) Gene expression regulation mediated through reversible $m^6A$ RNA methylation. *Nat Rev Genet* 15:293–306.
13. Xiao W, et al. (2016) Nuclear m(6)A reader YTHDC1 regulates mRNA splicing. *Mol Cell* 61:507–519.
14. Kane SE, Beemon K (1985) Precise localization of m6A in Rous sarcoma virus RNA reveals clustering of methylation sites: Implications for RNA processing. *Mol Cell Biol* 5:2298–2306.
15. Tirumuru N, et al. (2016) N(6)-methyladenosine of HIV-1 RNA regulates viral infection and HIV-1 Gag protein expression. *Elife* 5:e15528.
16. Lichinchi G, et al. (2016) Dynamics of the human and viral m(6)A RNA methylomes during HIV-1 infection of T cells. *Nat Microbiol* 1:16011.
17. Lichinchi G, et al. (2016) Dynamics of human and viral RNA methylation during Zika virus infection. *Cell Host Microbe* 20:666–673.
18. Kennedy EM, et al. (2016) Posttranscriptional m(6)A editing of HIV-1 mRNAs enhances viral gene expression. *Cell Host Microbe* 19:675–685.
19. Gokhale NS, et al. (2016) N6-methyladenosine in flaviviridae viral RNA genomes regulates infection. *Cell Host Microbe* 20:654–665.
20. Wan Y, et al. (2015) Transcriptome-wide high-throughput deep m(6)A-seq reveals unique differential m(6)A methylation patterns between three organs in Arabidopsis thaliana. *Genome Biol* 16:272.
21. Zhong S, et al. (2008) MTA is an Arabidopsis messenger RNA adenosine methylase and interacts with a homolog of a sex-specific splicing factor. *Plant Cell* 20:1278–1288.
22. Bodi Z, et al. (2012) Adenosine methylation in Arabidopsis mRNA is associated with the 3′ end and reduced levels cause developmental defects. *Front Plant Sci* 3:48.
23. Shen L, et al. (2016) N(6)-methyladenosine RNA modification regulates shoot stem cell fate in Arabidopsis. *Dev Cell* 38:186–200.
24. Mielecki D, et al. (2012) Novel AlkB dioxygenases—alternative models for in silico and in vivo studies. *PLoS One* 7:e30588.
25. van den Born E, et al. (2008) Viral AlkB proteins repair RNA damage by oxidative demethylation. *Nucleic Acids Res* 36:5451–5461.
26. Bol JF (2005) Replication of alfamo- and ilarviruses: Role of the coat protein. *Annu Rev Phytopathol* 43:39–62.
27. Herranz MC, Pallás V, Aparicio F (2012) Multifunctional roles for the N-terminal basic motif of Alfalfa mosaic virus coat protein: Nucleolar/cytoplasmic shuttling, modulation of RNA-binding activity, and virion formation. *Mol Plant Microbe Interact* 25: 1093–1103.
28. Ibrahim A, Hutchens HM, Berg RH, Loesch-Fries LS (2012) Alfalfa mosaic virus replicase proteins, P1 and P2, localize to the tonoplast in the presence of virus RNA. *Virology* 433:449–461.
29. Pallas V, Aparicio F, Herranz MC, Sanchez-Navarro JA, Scott SW (2013) The molecular biology of ilarviruses. *Adv Virus Res* 87:139–181.
30. Balasubramaniam M, Kim BS, Hutchens-Williams HM, Loesch-Fries LS (2014) The photosystem II oxygen-evolving complex protein PsbP interacts with the coat protein of Alfalfa mosaic virus and inhibits virus replication. *Mol Plant Microbe Interact* 27: 1107–1118.
31. Aparicio F, Pallás V (2017) The coat protein of Alfalfa mosaic virus interacts and interferes with the transcriptional activity of the bHLH transcription factor ILR3 promoting salicylic acid-dependent defence signalling response. *Mol Plant Pathol* 18:173–186.
32. Kumakura N, et al. (2009) SGS3 and RDR6 interact and colocalize in cytoplasmic SGS3/RDR6-bodies. *FEBS Lett* 583:1261–1266.
33. Martínez de Alba AE, et al. (2015) In plants, decapping prevents RDR6-dependent production of small interfering RNAs from endogenous mRNAs. *Nucleic Acids Res* 43: 2902–2913.
34. Ingelfinger D, Arndt-Jovin DJ, Lührmann R, Achsel T (2002) The human LSm1-7 proteins colocalize with the mRNA-degrading enzymes Dcp1/2 and Xrnl in distinct cytoplasmic foci. *RNA* 8:1489–1501.
35. Garcia D, Garcia S, Voinnet O (2014) Nonsense-mediated decay serves as a general viral restriction mechanism in plants. *Cell Host Microbe* 16:391–402.
36. Mérai Z, et al. (2013) The late steps of plant nonsense-mediated mRNA decay. *Plant J* 73:50–62.
37. Aparicio F, Sánchez-Navarro JA, Olsthoorn RC, Pallás V, Bol JF (2001) Recognition of cis-acting sequences in RNA 3 of Prunus necrotic ringspot virus by the replicase of Alfalfa mosaic virus. *J Gen Virol* 82:947–951.
38. Sánchez-Navarro JA, Reusken CB, Bol JF, Pallás V (1997) Replication of alfalfa mosaic virus RNA 3 with movement and coat protein genes replaced by corresponding genes of Prunus necrotic ringspot ilarvirus. *J Gen Virol* 78:3171–3176.
39. Luo G-Z, et al. (2014) Unique features of the m6A methylome in Arabidopsis thaliana. *Nat Commun* 5:5630.
40. Gregory BD, et al. (2008) A link between RNA metabolism and silencing affecting Arabidopsis development. *Dev Cell* 14:854–866.
41. Bratlie MS, Drabløs F (2005) Bioinformatic mapping of AlkB homology domains in viruses. *BMC Genomics* 6:1.
42. Bergua M (2011) El virus del mosaico de la alfalfa (AMV) en España: incidencia y efectos en alfalfa y análisis de la diversidad biológica y genética de poblaciones procedentes de distintos huéspedes. PhD thesis (Universidad de Zaragoza/Centro de Investigación y Tecnología Agroalimentaria de Aragón, Zaragoza, Spain).
43. Ryabov EV, Roberts IM, Palukaitis P, Taliansky M (1999) Host-specific cell-to-cell and long-distance movements of cucumber mosaic virus are facilitated by the movement protein of groundnut rosette virus. *Virology* 260:98–108.
44. Dominissini D, Moshitch-Moshkovitz S, Salmon-Divon M, Amariglio N, Rechavi G (2013) Transcriptome-wide mapping of N(6)-methyladenosine by m(6)A-seq based on immunocapturing and massively parallel sequencing. *Nat Protoc* 8:176–189.
45. Németh K, et al. (1998) Pleiotropic control of glucose and hormone responses by PRL1, a nuclear WD protein, in Arabidopsis. *Genes Dev* 12:3059–3073.
46. Aparicio F, Sánchez-Navarro JA, Pallás V (2006) In vitro and in vivo mapping of the Prunus necrotic ringspot virus coat protein C-terminal dimerization domain by bimolecular fluorescence complementation. *J Gen Virol* 87:1745–1750.
47. Pallás V, Más P, Sánchez-Navarro JA (1998) Detection of plant RNA viruses by non-isotopic dot-blot hybridization. *Methods Mol Biol* 81:461–468.
48. Martin M (2011) Cutadapt removes adapter sequences from high-throughput sequencing reads. *EMBnet.journal* 17:10–12.
49. Langmead B, Salzberg SL (2012) Fast gapped-read alignment with Bowtie 2. *Nat Methods* 9:357–359.
50. Robinson MD, Oshlack A (2010) A scaling normalization method for differential expression analysis of RNA-seq data. *Genome Biol* 11:R25.
51. Sievers F, et al. (2011) Fast, scalable generation of high-quality protein multiple sequence alignments using Clustal Omega. *Mol Syst Biol* 7:539.
52. Tamura K, Stecher G, Peterson D, Filipski A, Kumar S (2013) MEGA6: Molecular evolutionary genetics analysis version 6.0. *Mol Biol Evol* 30:2725–2729.
53. Saitou N, Nei M (1987) The neighbor-joining method: A new method for reconstructing phylogenetic trees. *Mol Biol Evol* 4:406–425.